DALTON
FULL PAPER

Copper complexes of the functionalised tripodal ligand tris(2-pyridyl)-methylamine and its derivatives †

Phillip J. Arnold,[a] Sian C. Davies,[b] Jonathan R. Dilworth,[c] Marcus C. Durrant,*[b] D. Vaughan Griffiths,[a] David L. Hughes,[b] Raymond L. Richards[d] and Philip C. Sharpe[a]

[a] *Department of Chemistry, Queen Mary and Westfield College, Mile End Road, London, UK E1 4NS*
[b] *Department of Biological Chemistry, John Innes Centre, Colney Lane, Norwich, UK NR4 7UH*
[c] *Inorganic Chemistry Laboratory, South Parks Road, Oxford, UK OX1 3QR*
[d] *School of Chemistry, Physics and Environmental Science, University of Sussex, Brighton, UK BN1 9QJ*

Received 20th October 2000, Accepted 18th January 2001
First published as an Advance Article on the web 13th February 2001

The coordination chemistry of the new tripodal ligand tris(2-pyridyl)methylamine (tpm) with copper(I), copper(II) and zinc(II) has been investigated. The synthesis of tpm can readily be modified to access a variety of related tripodal ligands such as 2-(methylsulfanyl)-1,1-di(2-pyridyl)ethylamine (mde); in addition, the primary amine function can be derivatised to extend further the range of complexes obtained. tpm itself is a versatile ligand, showing three distinct coordination modes: bidentate (py, NH_2), tridentate (2py, NH_2) and tridentate (3py). Complexes of stoichiometries $Cu(tpm)_n$ (n = 1–3) have been obtained. The (2py, NH_2) coordination mode is illustrated by the crystal structure of $[Cu(tpm)_2][BF_4]_2 \cdot Me_2CO$, whilst (3py) coordination is found in the crystal structures of $[Cu(SO_4)(tpm)(H_2O)] \cdot 3H_2O$, $[\{Cu(tpm)\}_2Br_3]Br \cdot 3MeOH$ and also the zinc complex $[Zn(tpm)(H_2O)_3]_2[Zn(H_2O)_6][SO_4]_3 \cdot 3H_2O$. Amide derivatives of tpm give complexes of stoichiometry CuL_2, and the crystal structures of $[Cu(tpma)_2][BF_4]_2$ [tpma = tris(2-pyridyl)methylacetamide] and $[Cu(tpms)_2] \cdot 8H_2O$ {tpmsH = 4-oxo-4-[tris(2-pyridyl)methylamino]-butanoic acid} have been determined. The crystal structure of the sulfate-bridged dimeric complex $[\{Cu(SO_4)(mde)\}_2] \cdot 3H_2O$ shows the mde ligand to be tridentate, with (2py, NH_2) coordination.

Introduction

Tripodal ligands based on nitrogen heterocycles have secured an important place in inorganic chemistry. The most extensive contributions to date have been made in the field of poly-pyrazolylborate coordination compounds, first prepared by Trofimenko in the 1960s.[1] In the last few years, however, other types of tripodal nitrogen ligand have received increasing attention, and the coordination chemistry of both tris-(pyrazolyl)methane[2] and tris(2-pyridyl)[3] ligands has recently been reviewed. It has been suggested that pyridine is both a better σ donor and a better π acid than pyrazole,[3] differences which should be reflected in the coordination chemistry of these various classes of ligand. The tris(2-pyridyl) ligands $(2\text{-}NC_5H_4)_3X$ reported to date encompass a very diverse selection of bridgehead groups X, including CH, COH, N, P, PO, As, Sn^{n}Bu and Pb.[3] Some of these ligands allow the possibility of elaboration of their coordination chemistry *via* derivatisation of the bridgehead group. For example, Levacher *et al.*[4] linked the carbinol $(2\text{-}NC_5H_4)_3COH$ to a polymeric support by derivatisation of the alcohol function to an ether; subsequent incorporation of iron gave a material which proved to be an efficient catalyst for methanolysis of styrene oxide. Recently, Jonas and Stack have commented on the versatility of this type of ligand and reported a systematic study of the copper coordination chemistry of the ligands $(2\text{-}NC_5H_4)_n[2\text{-}(6\text{-}MeO)C_5H_3N]_{(3-n)}\text{-}COMe$ (LOMe, n = 0 to 3).[5]

Our interests in this area stem from the identification by protein X-ray crystallography of the active site of copper-based nitrite reductase (NiR) as a so-called 'Type 2' copper site.[6–8] The coordination environment of Type 2 sites is provided by three histidine ligands from the protein plus one or more exogenous ligands. Similar sites are found in a wide variety of other metalloenzymes containing copper and/or zinc, in addition to NiR.[7,9] Type 2 copper centres are generally involved in catalysis and redox chemistry and typically have four- or five-coordinate copper in geometries ranging from tetrahedral, as in NiR,[6] to square pyramidal or trigonal bipyramidal.[10] The Type 2 copper in NiR is situated in a hydrophobic pocket, some 12 Å from the protein surface. In addition, the enzyme contains a 'Type 1' copper centre which mediates electron transfer to the active site.[8] The two copper centres are *ca.* 12.6 Å apart and linked directly through sequential histidine and cysteine residues. Derivatisable tripodal ligands offer the opportunity not only to model the immediate coordination environment of the Type 2 copper, but also to build in other features of the protein environment such as hydrophobicity or connections to a secondary metal centre. The theme of copper centres connected by nitrogen donor ligands has also been explored in the wider context of extended structural networks by the recent studies of Blake *et al.*[11]

We have focussed our efforts on the new ligand tris(2-pyridyl)-methylamine, tpm, and related species, and a preliminary account of our work has appeared.[12] The synthesis of tpm is readily modified to give a wide variety of related ligands, whilst the primary amine function is well suited for derivatisation and linking to other metal centres or solid supports. In this paper we set out the coordination chemistry of tpm and related species

† Electronic supplementary information (ESI) available: preparation and characterisation of amine derivative proligands. See http://www.rsc.org/suppdata/dt/b0/b008476j/

 DOI: 10.1039/b008476j

and their amine derivatives with copper. The crystal structures of six of the copper complexes and also a zinc complex of tpm are reported.

Results and discussion

The ligands used in this study are shown with their abbreviations in Scheme 1, and the physical and spectroscopic

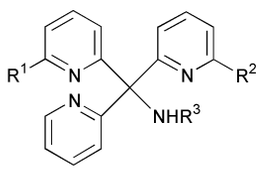

	R^1	R^2	R^3
tpm	H	H	H
bpm	Me	H	H
tpma	H	H	COMe
tpmI	H	H	$CO(CH_2)_{10}Me$
tpmsH	H	H	$CO(CH_2)_2CO_2H$
tpmbH	H	H	$CO(o\text{-}C_6H_4SO_3H)$
mopsH	OMe	H	$CO(CH_2)_2CO_2H$
bop	OMe	OMe	H
bopsH	OMe	OMe	$CO(CH_2)_2CO_2H$

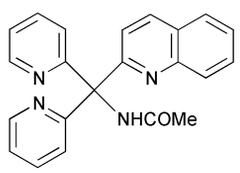

bpqa

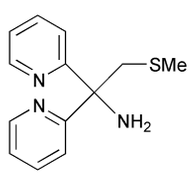

mde

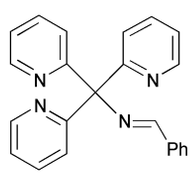

tpmSB

Scheme 1

properties of their complexes are given in Table 1 and the Experimental section. Most of the complexes contain solvent of crystallisation, sometimes in variable proportions depending on the procedure used to isolate the complex; this resulted in some differences between the solvent stoichiometries given in Table 1 and those determined by X-ray crystallography. The parent ligand, tris(2-pyridyl)methylamine, tpm, is readily prepared in 60% yield *via* a 'one pot' synthesis from 2-aminomethylpyridine and 2-chloropyridine. Variation of the reaction conditions allows isolation of the intermediate bis(2-pyridyl)-methylamine, previously prepared by reduction of the corresponding ketoxime,[13] from which a variety of other potential tripodal ligands are accessible. In all these compounds the primary amine group is readily converted into amide or Schiff base derivatives, which may themselves contain additional functional groups.

tpm itself exhibits three different coordination modes, two of which we have established by X-ray crystallography. The first is illustrated by the sulfato complex $[Cu(SO_4)(tpm)(H_2O)]\cdot 3H_2O$ **1** (Fig. 1), in which tpm is tridentate and coordinated through the three pyridine nitrogen atoms. Complex **1** has a distorted square pyramidal geometry, with a non-coordinated water occupying the sixth coordination site in octahedral geometry. Dimensions about the metal atom in this and the other complexes described below are listed in Table 2. In these crystals the Cu–tpm units bridge layers of hydrogen-bonded networks. The coordinated water molecule, O(5), and the sulfate ligand of the complex molecule are part of one hydrogen-bonded layer, and the tpm amine group links into the next layer. Within each layer there are alternative networks involving either the major components of the disordered sulfate and solvent molecules, or the minor components; a view of the major system is shown in Fig. 1(b).

It is likely that the complexes $[Cu(SO_4)(L)(H_2O)]\cdot nH_2O$ (L = bpm, **2**, L = bpqa, **3**) are structurally analogous to **1**. The tpm ligand in the bromide complex $[CuBr_2(tpm)]$ **4** probably also shares this coordination mode; **4** would then be analogous to the structurally characterised $[CuBr_2(Mepy_3CH)]$ ($Mepy_3CH$ = tris(6-methyl-2-pyridyl)methane).[14] Upon recrystallisation, complex **4** was converted into the bromide-bridged dimeric cation $[\{Cu(tpm)\}_2Br_3]^+$ **5**. Although the crystal structure of **5** showed significant disorder in the anion and solvent of crystallisation, the cation was well resolved (Fig. 2). One copper atom, Cu(2), is octahedrally coordinated by the three tpm pyridyl N atoms and three bromide ligands. The other is five-coordinate with a square pyramidal geometry; the Cu(1) · · · Br(1) distance is 2.980(4) Å, too long to be considered a bond. It appears, then, that the three *fac* bromide ligands cannot form triply bridging links between two copper atoms; as it is, there is a wide range of Cu–Br bonding distances, from 2.492(3) to 2.737(2) Å, in this complex. Difference peaks in this region suggest that in some cases the non-bridging bromide is replaced by a bridging methoxide ion with more equal bonding distances to the two copper atoms. The $Cu_2(\mu\text{-}X)_2$ structural motif is well established, but triple halide bridges to copper(II) are much rarer, and appear to be confined to date to catenated $[\{CuX_3\}_n]^{n-}$ species.[15] In the case of $[CuBr_2(Mepy_3CH)]$ the methyl groups probably provide sufficient steric hindrance to prevent formation of a dimer. In the structure of crystals of **5** the dimeric cation $[\{Cu(tpm)\}_2Br_3]^+$ lies on a mirror plane of symmetry and is elongated along the *c* axis, with the amine groups directed towards the mirror planes at $z = 1/4$ and 3/4. These planes, we believe, comprise networks of the anions and solvent molecules, linked to each other and to the amine groups by hydrogen bonds; the amine groups are hydrogen bonded to two of the three acceptor groups arranged in an almost equilateral triangle in the mirror plane. Each acceptor group comprises either a bromide ion (*ca.* 1/3 occupancy) or a solvent molecule (MeOH or H_2O, *ca.* 2/3 occupancy); the acceptor O atom of the solvent molecule was located in each case about 0.5 Å closer to the Br^- ion than to the amine N atom, but the associated methyl group was not resolved, perhaps disordered over several sites, hidden under the bromide peak or not present (*i.e.* the solvent is a water molecule). A separate group of three solvent atoms, each refined as a carbon atom, is probably a solvent (MeOH) molecule disordered over the three sites, in either direction, depending on the hydrogen bonds formed with neighbouring groups.

The second coordination mode of tpm is illustrated by the crystal structure of $[Cu(tpm)_2][BF_4]_2$ **6** (Fig. 3). Here the tpm ligands are also tridentate and tripodally coordinated, but the donor set comprises two pyridines and the primary amine. The amine hydrogen atoms in the tpm ligands of this complex were included in idealised positions and then allowed to refine freely. Both are involved in N–H · · · F hydrogen bonds to the disordered BF_4^- anions in either of two distinct orientations. The copper complex cations and the anions are thus linked in planar, hydrogen-bonded networks.

For both the (2py, NH_2) and (3py) tridentate coordination modes of tpm the three nitrogen atoms should form an equilateral triangle in ideal tripodal symmetry. Although all of the structurally characterised complexes in this study show some distortion from this ideal symmetry, the distortion is significantly increased for **6**; the three nitrogen donors form an approximate isosceles triangle with the largest angle (73.3°) subtended at the amine. This increased distortion is probably related to the fact that the bis(pyridine) amine coordination

Table 1 Colours, conductivities and analytical[a] data for the copper complexes

Complex	Colour	Λ_M[b]/S cm² mol⁻¹	Analysis (%)		
			C	H	N
1 $[Cu(SO_4)(tpm)(H_2O)]\cdot 2H_2O$	Blue	15 (MeCN + 20% water)	40.1 (40.4)	4.2 (4.2)	11.6 (11.8)
2 $[Cu(SO_4)(bpm)(H_2O)]\cdot 2H_2O$	Dark green	16 (MeOH)	41.7 (41.7)	4.4 (4.5)	11.3 (11.4)
3 $[Cu(SO_4)(bpqa)(H_2O)]\cdot 4H_2O$	Turquoise	2 (DMF)	43.7 (43.7)	4.3 (4.7)	9.1 (9.3)
4 $[CuBr_2(tpm)]\cdot 0.5H_2O$	Green	36 (DMF)	38.9 (38.8)	2.8 (3.1)	11.1 (11.3)
5 $[Cu_2Br_3(tpm)_2]Br\cdot 3H_2O$	Brown	87 (DMF)	37.0 (37.5)	3.2 (3.3)	10.9 (10.9)
6 $[Cu(tpm)_2][BF_4]_2\cdot C_3H_6O$	Blue	244 (MeCN)	51.4 (51.3)	4.3 (4.2)	13.7 (13.7)
7 $[Cu(tpm)_3][BF_4]_2$	Green	308 (MeCN)	56.0 (56.3)	4.1 (4.1)	16.4 (16.4)
8 $[Cu(OAc)_2(tpm)]\cdot 0.5CH_2Cl_2$	Green	56 (MeOH)	50.3 (50.6)	4.3 (4.4)	11.8 (11.5)
9 $[Cu(tpma)_2][BF_4]_2$	Lilac	292 (MeCN)	50.8 (51.1)	3.8 (3.8)	13.1 (13.2)
10 $[Cu(tpms)_2]\cdot 4H_2O$	Purple	13 (MeOH)	55.7 (56.0)	5.2 (4.9)	13.0 (13.1)
11 $[Cu(tpmb)_2]\cdot 3H_2O$	Lilac	13 (DMF)[c]	54.7 (54.8)	3.8 (4.0)	11.1 (11.1)
12 $[Cu(tpml)_2][BF_4]_2$	Purple	254 (MeCN)	59.3 (59.7)	6.5 (6.4)	9.9 (9.9)
13 $[Cu(SO_4)(tpml)(H_2O)]\cdot 0.5H_2O$	Light blue	0 (MeCN)	53.1 (53.3)	6.0 (6.2)	8.7 (8.9)
14 $[Cu_3(OAc)_4(mops)_2(H_2O)_2]\cdot CH_2Cl_2$	Turquoise	10 (MeCN + 10% water)	46.0 (46.0)	4.1 (4.2)	8.4 (8.4)
15 $[Cu(OAc)(bops)]\cdot 0.5CH_2Cl_2$	Blue	13 (MeOH)	49.9 (50.2)	4.3 (4.3)	9.8 (9.6)
16 $[Cu(OAc)(tpms)(H_2O)]$	Light blue	4 (DMF)	52.1 (52.6)	4.4 (4.4)	11.4 (11.2)
17 $[Cu_4(SO_4)_4(bop)_3]$	Light blue	51 (MeOH)	40.2 (40.4)	3.6 (3.4)	10.3 (10.5)
18 $[\{Cu(SO_4)(mde)\}_2]\cdot 2H_2O$	Blue	5 (MeOH)	36.9 (36.9)	4.0 (4.1)	9.5 (9.9)
19 $[Cu(SO_4)(mde)(H_2O)]\cdot 0.5H_2O$	Green	15 (MeOH)	35.8 (36.1)	3.8 (4.2)	9.7 (9.7)
21 $[Cu(tpm)(NCMe)]PF_6\cdot 0.33CH_2Cl_2$	Pale green	—	43.3 (43.3)	3.6 (3.8)	13.1 (13.1)

[a] Calculated values in parentheses. [b] Accepted ranges[24] for 1 : 1 and 1 : 2 electrolytes are as follows: DMF, 65–90 and 130–170 S cm² mol⁻¹ respectively; MeCN, 120–160 and 220–300 S cm² mol⁻¹ respectively; MeOH, 80–115 and 160–220 S cm² mol⁻¹ respectively. [c] Approximate value due to the complex's very poor solubility.

mode requires two 5- and one 6-membered chelate ring, whereas in the tris(pyridine) mode all three chelate rings are 6-membered. As expected, complex **6** exhibits Jahn–Teller distortion, but with the elongated axial sites occupied by two of the pyridines rather than the amine groups. This suggests that stronger bonding between the copper and the amino group compared to the pyridine nitrogens is offset by increased distortion of the coordination sphere required to coordinate the amine. Clearly, there is a fine balance between the tris-pyridine and bis-pyridine/amine donor sets in these complexes. The structure of complex **6** is closely related to that of $[Cu(dipa)_2][ClO_4]_2$ [dipa = bis(2-pyridyl)methylamine];[16] in this case also, two of the pyridine groups occupy the elongated axial positions. Interestingly, although $[Cu(dipa)_2]^{2+}$ and $[Cu(tpm)_2]^{2+}$ show very similar equatorial Cu–N distances (mean values 2.02 and 2.05 Å respectively), the axial Cu–N distances show a much greater variation (2.54 and 2.36 Å respectively). The relative weakness of these axial bonds probably makes them particularly susceptible to other influences, in this case perhaps the increased steric requirements of the bulkier tpm ligand compared to those of dipa.

Since complex **6** was initially isolated from the reaction of equimolar amounts of $Cu(BF_4)_2$ and tpm, we attempted a rational preparation using a higher ratio of tpm. However, the use of fairly concentrated reagent solutions led to precipitation of a new product, $[Cu(tpm)_3][BF_4]_2$ **7**. Assuming octahedral coordination, each of the ligands in this complex should be bidentate, giving a third coordination mode for tpm. Molecular models suggest that bidentate coordination can best be achieved *via* one pyridine and the amine; coordination through two pyridine rings is less likely not only on steric grounds, but also by virtue of the chelate effect, since in this arrangement the ligand is necessarily poised to become tridentate. It is worth noting here that the analogous ligands LOMe (see above) show bidentate coordination through two pyridines in the structurally characterised copper(I) complexes $[Cu(LOMe)_2][CF_3SO_3]$.[5] However, the steric requirements of two LOMe ligands in a tetrahedral arrangement should be significantly lower than those of three tpm ligands in an octahedral environment, as in complex **7**. Attempts to recrystallise **7** returned complex **6**.

Although use of $Cu(BF_4)_2$ as the copper starting material tends to give complexes of 1 : 2 or 1 : 3 rather than 1 : 1 metal: ligand stoichiometries, the converse is true for copper salts with more strongly coordinating anions, such as $CuSO_4$ and $CuBr_2$, as discussed above. Another example is provided by the acetato complex $[Cu(OAc)_2(tpm)]\cdot 0.5CH_2Cl_2$ **8**, whose conductivity (Table 1) suggests that both acetates remain coordinated in solution. The best pointer to the structure of this complex is probably the crystallographically characterised $[Cu(OAc)_2$-

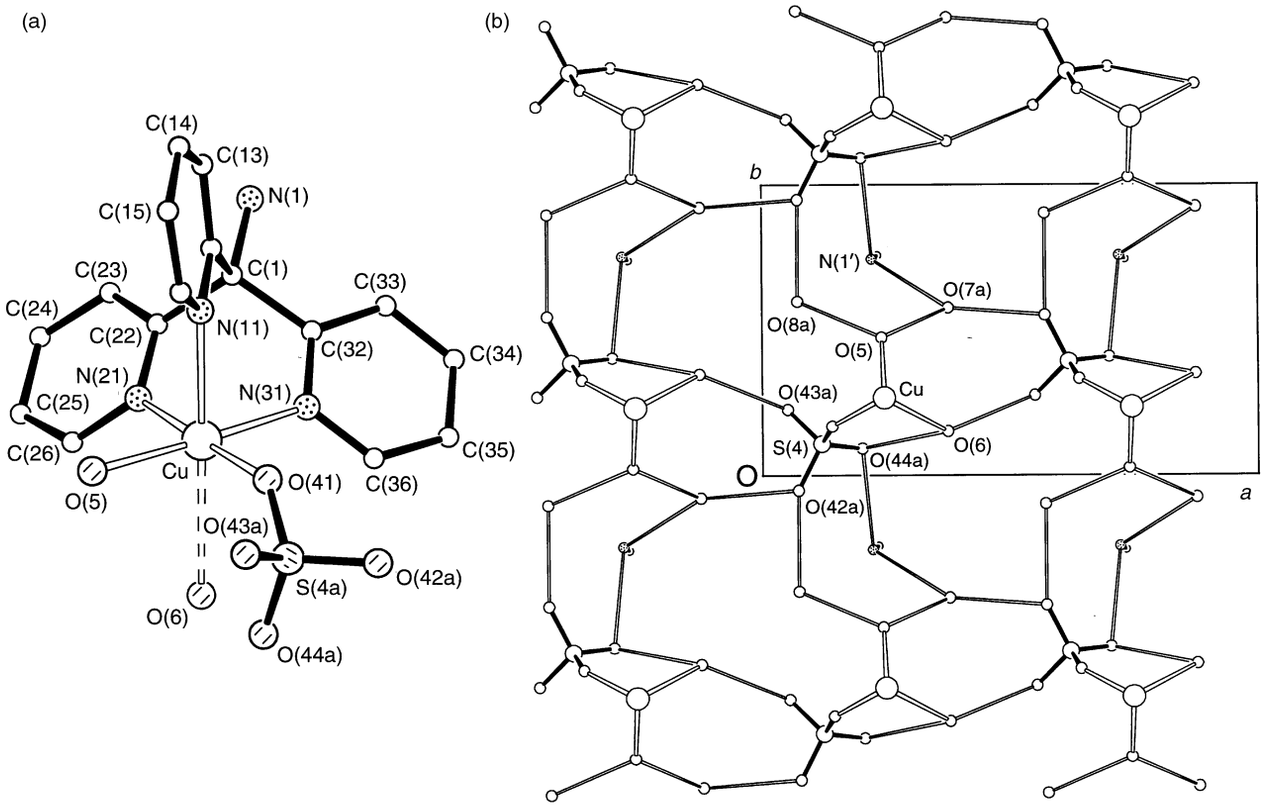

Fig. 1 Crystal structure of $[Cu(SO_4)(tpm)(H_2O)]\cdot 3H_2O$ **1**. The complex molecule is shown in (a) and a layer of the hydrogen bonding network, parallel to the *a*–*b* plane, in (b). In (b) the tpm ligand, which bridges the layers of hydrogen bond planes, is omitted for clarity. In all the molecular diagrams the atom numbering schemes are indicated and hydrogen atoms are omitted for clarity.

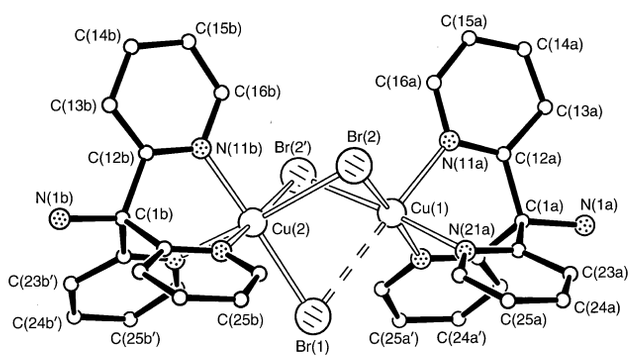

Fig. 2 Crystal structure of the cation of $[\{Cu(tpm)\}_2Br_3]Br\cdot 3MeOH$ **5**.

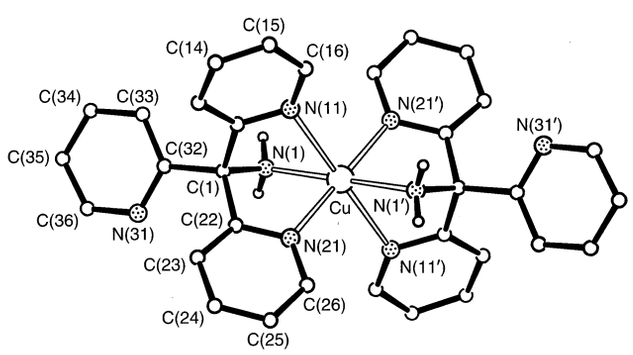

Fig. 3 Crystal structure of the cation of $[Cu(tpm)_2][BF_4]_2\cdot Me_2CO$ **6**.

$(py_2NH)]$, py_2NH = bis(2-pyridyl)amine,[17] in which the py_2NH ligand coordinates through the two pyridine nitrogens, whilst one acetato ligand is monodentate and the second is bidentate, giving distorted square-pyramidal coordination overall. The coordination sphere in complex **8** is probably similar, except that the tpm ligand is most likely tridentate.

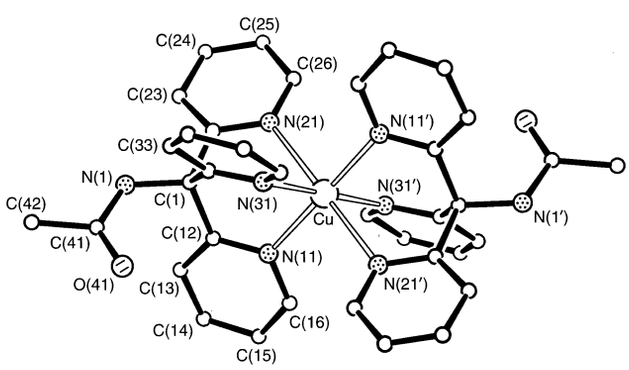

Fig. 4 Crystal structure of the cation of $[Cu(tpma)_2][BF_4]_2$ **9**.

Further control over the reaction products can be achieved by restricting the available coordination modes of the tpm ligand to the tris-pyridyl donor set, for example by derivatisation of the primary amine function to an amide. Structurally characterised examples of such complexes are provided by $[Cu(tpma)_2][BF_4]_2$ **9** and $[Cu(tpms)_2]\cdot 8H_2O$ **10** (Figs. 4 and 5 respectively). The copper atoms in these homoleptic complexes are in very similar Jahn–Teller distorted octahedral coordination environments. There is only one hydrogen atom available for forming hydrogen bonds in **9**, namely that of the amide group. This hydrogen links to a fluorine atom of the BF_4^- anion in either of its disordered orientations, thus forming discrete hydrogen-bonded $[Cu(tpma)_2][BF_4]_2$ units. Hydrogen atoms of all the solvent water molecules in complex **10** were located in difference maps and refined freely. These water molecules and the carboxylate oxygen atoms of the tpms ligands are linked by hydrogen bonds in layers, as shown in Fig. 5(b); the $[Cu(tpms)_2]$ molecules lie between, and bridge, these layers.

Reaction of the *ortho*-sulfonic acid derivative tpmbH with a variety of copper(II) starting materials produced in all cases the homoleptic complex $[Cu(tpmb)_2]$ **11**. The driving force for this

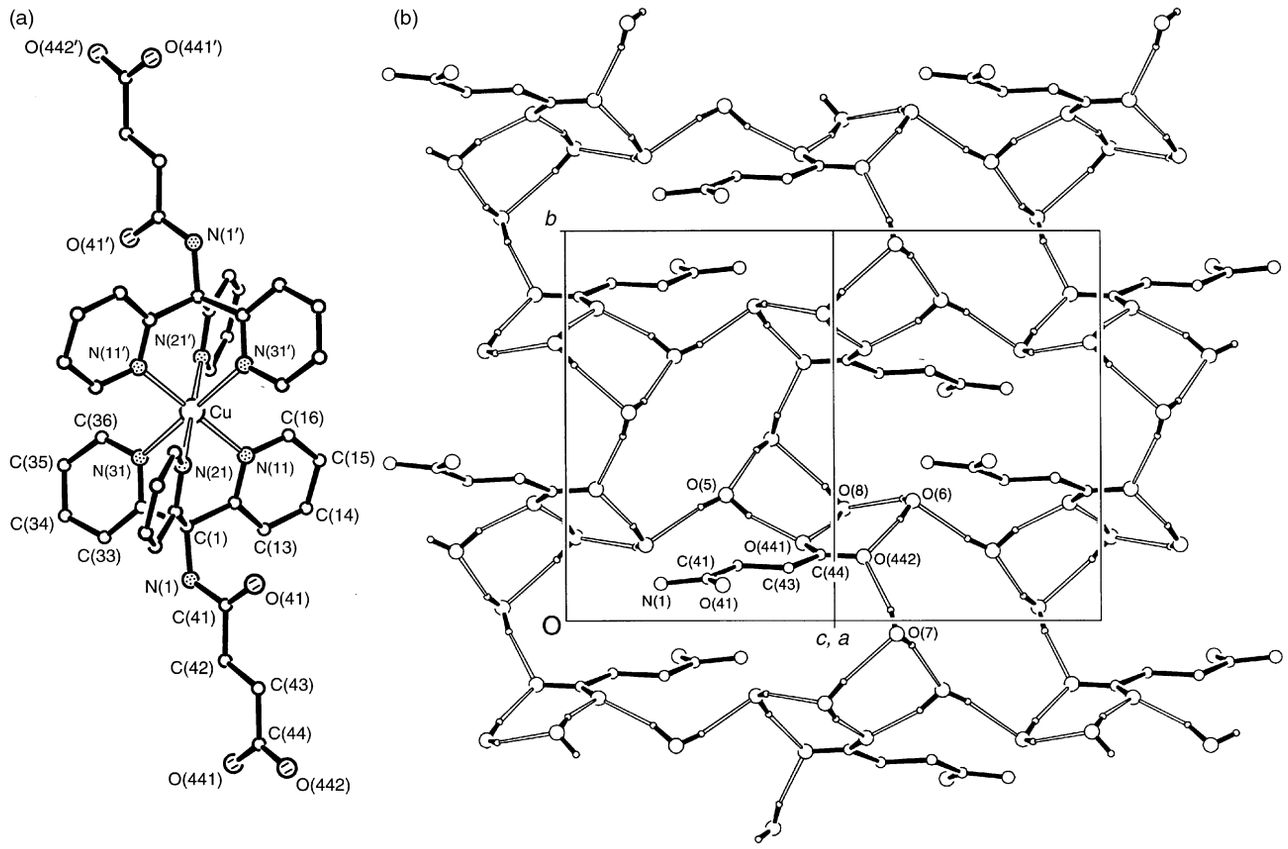

Fig. 5 Crystal structure of $[Cu(tpms)_2]\cdot 8H_2O$ **10**. The complex molecule is shown in (a), and a layer of the hydrogen bonding network, viewed down the (1 0 −1) axis, in (b). The copper and pyridine rings are omitted for clarity.

reaction is probably the very low solubility of **11** in all common solvents, including DMF and water. The anomalous chemical shifts of free tpmbH compared to the other tpm amides (see Experimental section) suggest that this compound may exist as its zwitterionic pyridinium sulfonate form in solution.

As an alternative to amide derivatisation, tpm can be converted into a Schiff base such as tpmSB (Scheme 1). This derivative proved less robust than the amides; thus, reaction of tpmSB with copper(II) sulfate gave the tpm complex **1** plus free benzaldehyde. However, we were able to prepare copper(II) nitrite complexes of Schiff base ligands of this type.[18]

Derivatisation of the tpm ligand can be used to modify the physical properties of the resulting complexes. Thus derivatisation of tpm with lauroyl chloride leads to complexes with significantly enhanced hydrophobicity, such as $[Cu(tpml)_2][BF_4]_2$ **12** and $[Cu(SO_4)(tpml)(H_2O)]$ **13**, which are readily soluble in solvents such as dichloromethane. Similarly, complex **9** is a 1:2 electrolyte whereas **10** is overall charge-neutral by virtue of its pendant carboxylate groups. The carboxylate groups in this kind of complex could in principle ligate a second metal atom; this would account for the stoichiometry of the trinuclear complex $[Cu_3(OAc)_4(mops)_2(H_2O)_2]$ **14**, in which a central $Cu(mops)_2$ unit probably links two $Cu(OAc)_2$ centres. The central copper could possess an N_6 coordination environment, similar to those of **9** and **10**; however, comparison of the colours of these complexes (Table 1) suggests that the structure shown in Scheme 2 is more likely. The two terminal copper atoms would then be structurally similar to those in complex **8**. Hence, these functionalised ligands allow the possibility of linking copper centres possessing different coordination environments.

As well as derivatisation of tpm before metal complexation, it proved possible to derivatise the amino group of coordinated tpm, even when this group is itself initially coordinated. For example, reaction of complex **6** with acetic anhydride gave the corresponding tpma complex **9**. The slow rate of this reaction

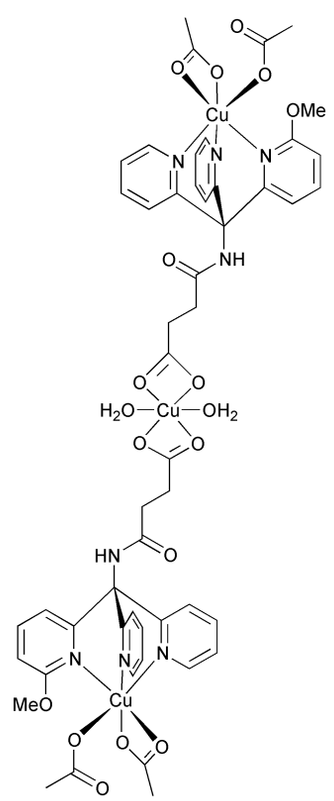

Scheme 2 Proposed structure of complex **14**.

at room temperature, requiring days compared to hours for free tpm, is presumably associated with the required change in the coordination mode of the ligand.

In addition to derivatisation of the amine function of tpm, substitution at the pyridine rings is also possible *via* modified

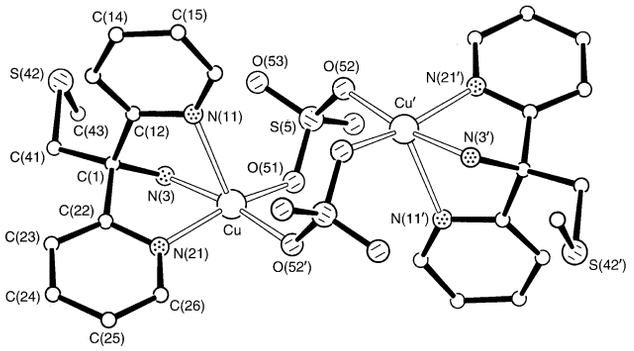

Fig. 6 Crystal structure of the dimer complex in $[\{Cu(SO_4)(mde)\}_2]\cdot 3H_2O$ **18**.

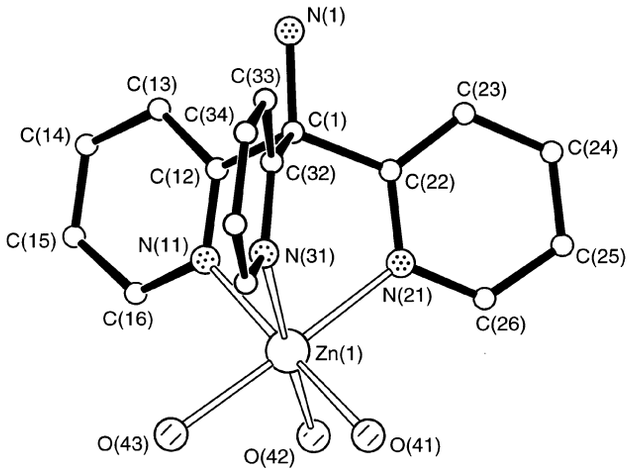

Fig. 7 Crystal structure of one of the two virtually identical tpm-containing cations of $[Zn(tpm)(H_2O)_3]_2[Zn(H_2O)_6][SO_4]_3\cdot 3H_2O$ **20**.

synthetic procedures. Such changes may give markedly different copper complexes. Thus, whilst [Cu(OAc)(bops)] **15** appears to be a direct analogue of [Cu(OAc)(tpms)(H_2O)] **16**, reaction of bop with $CuSO_4$ did not give an analogue of **1** but an apparently polynuclear complex, $[Cu_4(SO_4)_4(bop)_3]$ **17**. The thioether ligand mde (Scheme 1) gave two distinct complexes, both formulated as $Cu(SO_4)(mde)(H_2O)_n$, **18** and **19**. It appears that they do not interconvert in solution. Of the two, only **18** could be crystallised; the crystal structure (Fig. 6) shows a dimeric structure in which the mde ligands are tridentate, each coordinated *via* the two pyridine rings and the amine nitrogen, analogous to the second coordination mode of tpm discussed above. The two Cu(mde) units are bridged about a centre of symmetry by the two sulfate ligands. Of the two independent solvent water molecule sites in $[\{Cu(SO_4)(mde)\}_2]\cdot 3H_2O$, **18**, one appears to be only half occupied. The hydrogen atoms of the water molecule in the fully occupied site and of the amine ligand were located and refined, and all form hydrogen bonds so that the dimer molecules are linked in sheets through the crystal. The sheets are linked only by rather weaker hydrogen bonds through the partial-occupancy water molecules.

Comparison of all of the structurally characterised copper(II) complexes obtained in this work reveals a common distortion in which the plane of the coordinated pyridine ring deviates from the ideal orientation parallel to the Cu–N bond vector. This can be quantified by the angle formed between the Cu–N bond and the N–C diagonal of the pyridine ring, ideal value 180°. The greatest distortion is found in complex **6**, where one of these angles is 158.1(1)°. This phenomenon probably originates in the Jahn–Teller effect, since it appears to be absent in the zinc cations $[Zn(tpm)(H_2O)_3]^{2+}$ **20** [Fig. 7; Zn–N–C angles 172.1(2)–178.0(2)°]. There are two distinct $[Zn(tpm)(H_2O)_3]^{2+}$ cations and one $[Zn(H_2O)_6]^{2+}$ cation in the crystal, and these are arranged in layers parallel to the *a*–*b* plane: layer I, at $z = 0$, comprises cations of the first type, namely the cation of Zn(1); layer II, about $z = ½$, is a very similar layer of the second, Zn(2), cation. These cations are separated by layer III, at $z = ¼$ and ¾, which comprises the Zn(3) $[Zn(H_2O)_6]^{2+}$ cations, the sulfate anions and the water molecules. Layer III is an extensively hydrogen-bonded system linking all moieties and involving, also, all the coordinated water molecules and the tpm amine groups. Each cation in layers I and II bridges two layers III, with its water ligands in one layer III and its amine group in the next. The extensive hydrogen bonding might account for the preservation of the stoichiometry of this complex on recrystallisation.

The diamagnetic copper(I) complex $[Cu(tpm)(NCMe)]PF_6$ **21** proved highly air-sensitive in solution, frustrating attempts at crystallisation. This contrasts with the related tris(pyrazolylmethane) complexes $[Cu(HC\{3\text{-}Rpz\})(NCMe)]PF_6$, which are described as 'moderately air-stable even as solutions',[2] and is possibly due to the more open nature of the copper site in **21**. Based on the NMR data, complex **21** is probably tetrahedral, with a tris-pyridyl donor set for the tpm ligand. The crystal structures of analogous complexes $[Cu(LOMe)(NCMe)][CF_3SO_3]$ have recently been reported.[5]

Free tpm shows the characteristic pyridine π–π* absorption at 263 nm in acetonitrile solution. This band is essentially unchanged in position, but increased in intensity, in the spectra of all the complexes (see Experimental section). The relatively weak copper(II) d–d band ranges from 570 to 715 nm. The IR spectra of tpm and its amide derivatives show weak bands at 3200–3400 cm^{-1} associated with ν(NH) (see Experimental section). These bands are generally also present in the spectra of the complexes, unless obscured by water of crystallisation. The amide I band appears at 1630–1695 cm^{-1} for the free amides and their complexes. Although the carbonyl group is not involved in coordination, the band generally shows a significant shift to higher wavenumbers in the spectra of the complexes. The shift presumably has its origin in the overall electronic state of the ligand, since it is larger for the anionic ligand tpms$^-$ (50–60 cm^{-1}) than the neutral ligands tpma and tpml (20–35 cm^{-1}). tpmbH again provides the exception, with the amide I band shifted to *lower* wavenumbers by 14 cm^{-1} for complex **11** compared to the "free" ligand. This may be associated with an internal hydrogen bond between the amide NH and the sulfonate group. The pyridine rings give medium intensity bands at 1530–1600 cm^{-1}, which generally show small shifts (maximum 12 cm^{-1}) to higher wavenumbers on coordination. Whereas $[Cu(tpma)_2][BF_4]_2$ **9** shows two such bands, $[Cu(tpm)_2][BF_4]_2$ **6** gives three and $[Cu(tpm)_3][BF_4]_2$ **7** four, presumably a consequence of the presence of both coordinated and non-coordinated pyridine rings in the last two complexes. All of the ligands and their complexes show a variable number of generally sharp, medium intensity bands below 1200 cm^{-1}, highly characteristic of the individual compound but of little diagnostic value. The SO_4^{2-}, BF_4^- and PF_6^- anions give characteristic strong IR features.

Conclusion

tpm and its substituted derivatives constitute a versatile new class of tripodal ligands for copper and other metals. The synthetic procedures described in this work can readily be extended to give compounds incorporating one or more substituted pyridines, or indeed completely different functional groups such as thioethers. An entirely separate approach to derivatisation is provided by the primary amine function. Conversion of this group into an amide, Schiff base or other derivative can be used to tune the properties of the resulting complexes such as charge, solubility, *etc.* Such derivatisation may be carried out before or after complexation to the metal. Incorporation of further functional groups in this way can be used to link the

Table 2 Bond lengths (Å) and angles (°) about the metal atoms in the copper and zinc complexes

$[Cu(SO_4)(tpm)(H_2O)]\cdot 3H_2O$ **1**		$[\{Cu(mde)(SO_4)\}_2]\cdot 3H_2O$ **18**		$[\{Cu(tpm)\}_2Br_3]Br\cdot 3MeOH$ **5**			
Cu–N(11)	2.192(5)	Cu–N(11)	2.336(4)	Cu(1)–N(11a)	2.134(13)	Cu(2)–N(11b)	2.034(13)
Cu–N(21)	2.017(5)	Cu–N(21)	2.027(4)	Cu(1)–N(21a)	2.060(10)	Cu(2)–N(21b)	2.099(10)
Cu–N(31)	2.019(5)	Cu–N(3)	1.980(4)	Cu(1)···Br(1)	2.980(4)	Cu(2)–Br(1)	2.492(3)
Cu–O(41)	1.941(5)	Cu–O(51)	1.959(3)	Cu(1)–Br(2)	2.508(2)	Cu(2)–Br(2)	2.737(2)
Cu–O(5)	2.018(6)	Cu–O(52′)	1.940(3)	Cu(1)–O(1x)	2.135(2)	Cu(2)–O(1x)	2.199(2)
Cu–O(6)	2.658(10)			O(1x)–C(1x)	1.57(4)		
Angles subtended at Cu							
N(21)/N(11)	87.4(2)	N(11)/N(21)	85.9(2)	N(11a)/N(21a)	87.4(4)	N(11b)/N(21b)	84.7(4)
N(31)/N(11)	85.8(2)	N(11)/N(3)	73.7(2)	Br(2)/N(11a)	97.0(3)	Br(1)/N(11b)	177.8(4)
O(41)/N(11)	92.3(2)	N(11)/O(51)	108.68(14)	N(21a)/N(21a′)	85.3(5)	Br(2)/N(11b)	92.5(3)
O(5)/N(11)	93.6(2)	N(11)/O(52′)	113.04(14)	Br(2)/N(21a)	93.2(3)	N(21b)/N(21b′)	88.2(5)
N(21)/N(31)	85.6(2)	N(21)/N(3)	80.2(2)	Br(2)/N(21a′)	175.3(3)	Br(1)/N(21b)	93.8(3)
O(41)/N(21)	177.4(2)	N(21)/O(51)	160.5(2)	Br(2)/Br(2′)	87.94(10)	Br(2)/N(21b)	96.3(3)
N(21)/O(5)	91.3(2)	N(21)/O(52′)	94.2(2)	N(11a)/O(1x)	175.4(4)	Br(2)/N(21b′)	174.4(3)
O(41)/N(31)	91.8(2)	N(3)/O(51)	91.4(2)	N(21a)/O(1x)	96.0(3)	Br(1)/Br(2)	89.23(8)
O(5)/N(31)	176.9(2)	N(3)/O(52′)	171.1(2)	O(1x)/Br(2)	79.74(7)	Br(2)/Br(2′)	78.99(9)
O(41)/O(5)	91.3(2)	O(51)/O(52′)	91.8(2)			N(11b)/O(1x)	161.8(4)
						N(21b)/O(1x)	108.1(3)
						O(1x)/Br(2)	73.65(6)
$[Cu(tpm)_2][BF_4]_3\cdot Me_2CO$ **6**		$[Cu(tpma)_2][BF_4]_2$ **9**		$[Cu(tpms)_2]\cdot 8H_2O$ **10**			
Cu–N(11)	2.360(3)	Cu–N(11)	2.027(4)	Cu–N(11)	2.006(2)		
Cu–N(21)	2.041(2)	Cu–N(21)	2.357(4)	Cu–N(21)	2.033(2)		
Cu–N(1)	2.063(2)	Cu–N(31)	2.003(4)	Cu–N(31)	2.342(2)		
Angles subtended at Cu							
N(11)/N(21)	88.95(8)	N(11)/N(21)	86.7(2)	N(11)/N(21)	85.81(7)		
N(11)/N(1)	72.10(9)	N(31)/N(11)	86.1(2)	N(11)/N(31)	84.07(7)		
N(21)/N(1)	77.26(9)	N(31)/N(21)	83.3(2)	N(21)/N(31)	87.37(7)		
$[Zn(tpm)(H_2O)_3]_2[Zn(H_2O)_6][SO_4]_3\cdot 3H_2O$ **20**							
Zn(1)–N(11)	2.111(3)	Zn(2)–N(51)	2.118(3)	Zn(3)–O(81)	2.106(3)		
Zn(1)–N(21)	2.131(3)	Zn(2)–N(61)	2.135(3)	Zn(3)–O(82)	2.140(3)		
Zn(1)–N(31)	2.137(3)	Zn(2)–N(71)	2.139(4)	Zn(3)–O(83)	2.156(3)		
Zn(1)–O(41)	2.094(4)	Zn(2)–O(44)	2.099(3)	Zn(3)–O(84)	2.063(3)		
Zn(1)–O(42)	2.090(3)	Zn(2)–O(45)	2.095(4)	Zn(3)–O(85)	2.076(3)		
Zn(1)–O(43)	2.112(4)	Zn(2)–O(46)	2.094(4)	Zn(3)–O(86)	2.060(3)		
Angles subtended at the Zn atoms							
N(11)/N(21)	86.02(13)	N(51)/N(61)	85.43(13)	O(81)/O(82)	178.32(13)		
N(11)/N(31)	83.83(13)	N(51)/N(71)	85.05(13)	O(81)/O(83)	93.70(14)		
O(41)/N(11)	176.1(2)	O(44)/N(51)	92.17(13)	O(84)/O(81)	92.77(14)		
O(42)/N(11)	92.46(14)	O(45)/N(51)	92.59(14)	O(85)/O(81)	85.91(14)		
N(11)/O(43)	91.3(2)	O(46)/N(51)	177.9(2)	O(86)/O(81)	92.9(2)		
N(21)/N(31)	83.86(13)	N(61)/N(71)	83.37(13)	O(82)/O(83)	87.97(13)		
O(41)/N(21)	93.5(2)	O(44)/N(61)	89.59(14)	O(84)/O(82)	87.44(13)		
O(42)/N(21)	92.15(13)	O(45)/N(61)	177.7(2)	O(85)/O(82)	92.44(12)		
O(43)/N(21)	177.28(14)	O(46)/N(61)	92.5(2)	O(86)/O(82)	86.99(13)		
O(41)/N(31)	92.3(2)	O(44)/N(71)	172.61(14)	O(84)/O(83)	87.41(14)		
O(42)/N(31)	174.72(14)	O(45)/N(71)	95.3(2)	O(85)/O(83)	175.27(13)		
O(43)/N(31)	96.03(14)	O(46)/N(71)	94.3(2)	O(86)/O(83)	89.82(14)		
O(42)/O(41)	91.4(2)	O(45)/O(44)	91.6(2)	O(84)/O(85)	87.90(13)		
O(41)/O(43)	89.2(2)	O(46)/O(44)	88.3(2)	O(86)/O(84)	173.86(14)		
O(42)/O(43)	87.79(14)	O(46)/O(45)	89.4(2)	O(86)/O(85)	94.91(14)		

complexes to secondary metal centres, or to solid supports such as polymers, in principle allowing coupling of a catalytic site to an electron transfer centre.

The penalty for such flexibility in ligand design is the unpredictability of the resulting coordination chemistry. The variability of copper coordination chemistry is highlighted both in the present study and in literature reports on related systems. As well as the principles of ligand design emerging from this and other studies, use of coordinating anions such as sulfate can help to control complex formation. With respect to copper-based nitrite reductase, our next report in this area will deal with the preparation and characterisation of copper nitrite complexes of these ligands.

Experimental

Copper(II) compounds were prepared under air, other species under nitrogen. $[Cu(NCMe)_4]PF_6$ was prepared by the literature procedure.[19] Infrared (400–4600 cm^{-1}, Nujol mulls) and UV-vis (200–800 nm) spectra were recorded using Shimadzu FTIR-8300 and UV-2101PC spectrophotometers respectively. ^1H, ^{13}C and ^{31}P NMR spectra were recorded at 270.17, 67.94 and 109.38 MHz respectively using a JEOL GSX270 spectrometer and chemical shifts are quoted relative to external $SiMe_4$ or $P(OMe)_3$ (note superscripts used below in the ^1H and ^{13}C assignments refer to the heterocyclic rings). Melting points and solution conductivities were obtained using an Electrothermal melting-point apparatus and a Portland Electronic conductivity meter respectively. Microanalyses were determined by Mr. A. Saunders (University of East Anglia). Electron impact mass spectra were obtained at 8 keV on a Kratos MS50TC instrument at Queen Mary and Westfield College, FABS mass spectra by Dr M. Cocksedge at the ULIRS Mass Spectrometry Facility, London. Details of the preparation and

characterisation of the amine derivative proligands have been deposited as ESI.

Preparations

Tris(2-pyridyl)methylamine, tpm, 1,1-bis(6-methoxy-2-pyridyl)-1-(2-pyridyl)methylamine, bop, and bis(2-pyridyl)-methylamine. A solution of 2-aminomethylpyridine (10.8 g, 100 mmol) in dry THF (110 cm^3) was cooled to −78 °C under N_2 and n-butyllithium (40 cm^3 of 2.5 M solution in hexane, 100 mmol) added dropwise. The mixture was allowed to rise slowly to room temperature and stirred for 24 h. 2-Chloropyridine (11.4 g, 100 mmol) was added dropwise and the mixture stirred for 24 h. Water (30 cm^3) was added and the mixture stirred for 30 min. The volatile components were removed *in vacuo* and the residue was partitioned between CH_2Cl_2 and water. The layers were separated and the aqueous layer was extracted with CH_2Cl_2. The organic layers were combined, dried over $MgSO_4$ and reduced *in vacuo*. The resulting oil was triturated with Et_2O–hexane (1:1) to give a solid, which was recrystallised from near-boiling water as tpm (7.8 g, 60%). (Found: C, 73.1; H, 5.3; N, 21.2. Calc. for $C_8H_7N_2$: C, 73.3; H, 5.4; N, 21.4%). mp 98 °C. ^{1}H NMR (CD_2Cl_2): δ 8.53 (m, 3H, H^6), 7.62 (m, 3H, H^4), 7.35 (m, 3H, H^3), 7.17 (m, 3H, H^5) and 3.34 (br s, 2H, exchanges with D_2O, NH_2). ^{13}C NMR (CD_2Cl_2): δ 165.6 (s, C^2), 148.8 (d, J_{CH} = 178, C^6), 136.3 (d, J_{CH} = 161, C^4), 123.4 (d, J_{CH} = 168, C^3), 122.1 (d, J_{CH} = 164 Hz, C^5) and 70.6 (s, CNH_2). IR: 3362w and 3294w (NH_2), 1583m and 1568m (py ring), 1148m, 993m, 876m, 772m, 746m, 660m, 619m and 586m cm^{-1}. UV (MeCN): 263 nm (ε 9580 M^{-1} cm^{-1}).

A similar procedure, using 2-chloro-6-methoxypyridine in place of 2-chloropyridine, gave after recrystallisation from Et_2O–hexane, bop in 17% yield (Found: C, 67.2; H, 5.6; N, 17.2%; M^+, *m/z* 322.1432. Calc. for $C_9H_9N_2O$: C, 67.1; H, 5.6; N, 17.4%; *m/z* 322.1430). mp 75 °C. ^{1}H NMR ($CDCl_3$): δ 8.56 (m, 1H, H^6), 7.58 (m, 1H, H^4), 7.50 (m, 2H, $H^{4'}$), 7.30 (m, 1H, H^3), 7.13 (m, 1H, H^5), 6.91 (m, 2H, $H^{3'}$), 6.60 (m, 2H, $H^{5'}$), 3.74 (s, 6H, CH_3) and 3.37 (br s, 2H, NH_2). ^{13}C-{^{1}H} NMR ($CDCl_3$): δ 165.4 (C^2), 162.9 ($C^{6'}$), 161.1 ($C^{2'}$), 148.4 (C^6), 138.7 ($C^{4'}$), 135.6 (C^4), 123.4 (C^5), 121.6 (C^3), 115.8 ($C^{5'}$), 108.8 ($C^{3'}$), 69.9 (CNH_2) and 53.0 (CH_3). IR: 3364m and 3294m (NH_2), 3067w, 2943m, 2905w, 2851w, 1574s and 1563m (py ring), 1466s, 1427s, 1312s, 1261s, 1211m, 1169m, 1150w, 1119w, 1072w, 1030m, 988m, 907m, 849w, 799m, 764m, 698w and 602m cm^{-1}.

Use of the same quantities and procedure, except that the 2-chloropyridine was added over 20 min and the water quench added after stirring for 20 min rather than 24 h, gave bis(2-pyridyl)methylamine as a yellow oil (20.3 g, 43%). bp 85 °C at 0.03 Torr (lit.[13] 147–151 °C at 0.57 Torr). Spectroscopic properties as reported.[13]

Bis(2-pyridyl)-1-(2-quinolyl)methylamine, bpq, and 2-(methylsulfanyl)-1,1-bis(2-pyridyl)ethylamine, mde. A solution of bis(2-pyridyl)methylamine (1.5 g, 8.1 mmol) in dry THF (30 cm^3) was cooled to −78 °C under N_2 and n-butyllithium (4.8 cm^3, 2.5 M, 8.1 mmol) added dropwise. The mixture was allowed to warm slowly to room temperature and stirred for 2 h. 2-Chloroquinoline (1.3 g, 8.1 mmol) in dry THF (5 cm^3) was added dropwise (with care) and the mixture stirred for 24 h. Water (20 cm^3) was added and the layers were separated. The aqueous layer was extracted with CH_2Cl_2. The organic layers were combined, dried over $MgSO_4$ and reduced *in vacuo.* The residue was purified by column chromatography using silica and ethyl acetate, then recrystallised from CH_2Cl_2 as bpq (1.2 g, 47%). (Found: M^+, *m/z* 312.1375. $C_{20}H_{16}N_4$ requires 312.1375). mp 82 °C. ^{1}H NMR ($CDCl_3$): δ 8.56 (m, 2H, H^6), 8.03 (m, 2H, $H^{4'/8'}$), 7.64 (m, 2H, H^4), 7.56 (m, 1H, $H^{5'}$), 7.45 (m, 2H, H^3), 7.43−7.67 (m, 3H, $H^{3'/6'/7'}$), 7.13 (m, 2H, H^5) and 3.51 (br s, 2H, NH_2). ^{13}C-{^{1}H} NMR ($CDCl_3$): δ 165.1 (C^2), 164.4 (C^2), 148.6 (C^6), 146.9 ($C^{9'}$), 136.1 (C^4), 135.3 ($C^{8'}$), 129.4 ($C^{4'}$), 129.0 ($C^{7'}$), 127.2 ($C^{5'}$), 126.9 ($C^{10'}$), 126.2 ($C^{6'}$), 123.0 (C^3), 121.9 ($C^{3'}$), 121.7 (C^5) and 70.7 (CNH_2). IR: 3353w and 3283m (NH_2), 3051w, 3001w, 2929w, 1578m and 1585m (py ring), 1501m, 1462m, 1431m, 1308m, 1123w, 995m, 957w, 887w, 837m, 778m and 752m cm^{-1}. The preparation of bpqa from bpq is given as ESI.†

A similar procedure, using chloromethyl methyl sulfide in place of 2-chloroquinoline, gave after chromatography using silica–ethyl acetate, mde in 67% yield (Found: $[M+H]^+$, *m/z* 246.1080. Calc. for $C_{13}H_{16}N_3S$: 246.1065). ^{1}H NMR ($CDCl_3$): δ 8.53 (m, 2H, H^6), 7.54–7.64 (m, 2H, H^4), 7.49–7.53 (m, 2H, H^3), 7.05–7.15 (m, 2H, H^5), 3.63 (s, 2H, CH_2), 3.27 (br s, 2H, NH_2) and 1.89 (s, 3H, CH_3). ^{13}C-{^{1}H} NMR ($CDCl_3$): δ 163.6 (C^2), 148.0 (C^6), 136.0 (C^4), 121.5 (C^3), 121.2 (C^5), 64.6 (CNH_2), 47.3 (CH_2) and 17.1 (CH_3). IR: 3367w and 3296w (NH_2), 3053m, 3003m, 2916, 1587m and 1568m (py ring), 1463m, 1429m, 1151w, 995m, 750m, 650m and 619m cm^{-1}.

(6-Methoxy-2-pyridyl)bis(2-pyridyl)methylamine, mop and (6-methyl-2-pyridyl)bis(2-pyridyl)methylamine, bpm. A solution of bis(2-pyridyl)methylamine (2.0 g, 10.8 mmol) in dry THF (40 cm^3) was cooled to −78 °C under N_2 and n-butyllithium (4.3 cm^3, 2.5 M, 10.8 mmol) added dropwise. The mixture was allowed to warm slowly to room temperature and stirred for 4 h. 2-Chloro-6-methoxypyridine (1.55 g, 10.8 mmol) was added dropwise (with care) and the mixture heated under reflux for 18 h. Once cool, water (15 cm^3) was added and the mixture reduced to dryness *in vacuo*. The residue was taken up in CH_2Cl_2 and the solution was washed with water, dried over $MgSO_4$ and reduced *in vacuo*. The product was purified by column chromatography on silica using ethyl acetate–MeOH (200:3) as eluent to give a red oil characterised as mop (2.6 g, 84%). (Found: M^+, *m/z* 292.1324. Calc. for $C_{17}H_{16}N_4O$: 292.1324). ^{1}H NMR ($CDCl_3$): δ 8.54 (m, 2H, H^6), 7.55 (m, 2H, H^4), 7.48 (m, 1H, $H^{4'}$), 7.33 (m, 2H, H^3), 7.10 (m, 2H, H^5), 6.91 (m, 1H, $H^{3'}$), 6.58 (m, 1H, $H^{5'}$), 3.71 (s, 3H, CH_3) and 3.41 (br s, 2H, NH_2). ^{13}C-{^{1}H} NMR ($CDCl_3$): δ 164.9 (C^2), 162.6 ($C^{6'}$), 161.7 ($C^{2'}$), 148.3 (C^6), 138.5 ($C^{4'}$), 135.6 (C^4), 122.9 (C^5), 121.4 (C^3), 115.4 ($C^{5'}$), 108.6 ($C^{3'}$), 69.8 (CNH_2) and 52.7 (CH_3). The preparation of mops from mop is given as ESI.†

A similar procedure, using 2-chloro-6-methylpyridine in place of 2-chloro-6-methoxypyridine, gave, after recrystallisation of the crude product from Et_2O–hexane, bpm in 61% yield (Found: $[M + H]^+$, *m/z* 277.1464. Calc. for $C_{17}H_{18}N$: 277.1453). mp 54 °C. ^{1}H NMR ($CDCl_3$): δ 8.56 (m, 2H, H^6), 7.61 (m, 2H, H^4), 7.47 (m, 1H, $H^{4'}$), 7.40 (m, 2H, H^3), 7.13 (m, 2H, H^5), 7.01 (m, 2H, $H^{3'/5'}$), 2.86 (br s, 2H, NH_2) and 2.49 (s, 3H, CH_3). ^{13}C-{^{1}H} NMR ($CDCl_3$): δ 165.5 (C^2), 163.3 ($C^{2'}$), 157.3 ($C^{6'}$), 148.6 (C^6), 136.0 ($C^{4/4'}$), 123.0 (C^3), 121.6 (C^5), 121.3 ($C^{3'}$), 120.2 ($C^{5'}$), 70.1 (CNH_2) and 24.5 (CH_3). IR: 3368w and 3302w (NH_2), 3051w, 2924w, 1686w, 1585m (py ring), 1508w, 1458m, 1431m, 1319w, 1123w, 995m, 775w and 748m cm^{-1}.

$[Cu(SO_4)(tpm)(H_2O)]\cdot 2H_2O$ 1, $[Cu(SO_4)(bpm)(H_2O)]\cdot 2H_2O$ 2 and $[Cu(SO_4)(bpqa)(H_2O)]\cdot 4H_2O$ 3. A solution of $CuSO_4\cdot 5H_2O$ (0.47 g, 1.9 mmol) in water (5 cm^3) was added to a solution of tpm (0.50 g, 1.9 mmol) in ethanol (10 cm^3). The mixture was kept until most of the solvent had evaporated; the resulting crystalline precipitate was filtered off, washed with ethanol, and dried *in vacuo* as $[Cu(SO_4)(tpm)(H_2O)]\cdot 2H_2O$ **1** (0.65 g, 73%). IR (KBr disc): 3341s, br (H_2O), 1593m (py ring), 1467m, 1442m, 1116s, br (SO_4), 1053m, 976m, 781m, 759m, 653m, 507w, 435w and 421w cm^{-1}. UV–VIS (MeCN + 10% water): 656 (71) and 263 nm (ε 12500 M^{-1} cm^{-1}). Slow evaporation of a methanol–water solution of complex **1** in an open tube gave crystals suitable for X-ray diffraction.

A similar procedure using bpm rather than tpm gave, after trituration of the precipitate with acetone, $[Cu(SO_4)(bpm)(H_2O)]\cdot 2H_2O$ **2** in 84% yield. IR: *ca.* 3373m, br (H_2O), 1591m

and 1570m (py ring), 1304w, 1113s, br (SO_4), 1026s, 966m, 773m, 721m and 610m cm^{-1}. UV–VIS (MeOH): 664 (79), 358sh (1650) and 263 nm (ε 15000 M^{-1} cm^{-1}).

Likewise use of bpqa gave $[Cu(SO_4)(bpqa)(H_2O)]\cdot 4H_2O$ **3** in 23% yield. IR: *ca.* 3363m, br (H_2O), 1680m (amide I), 1599m (py ring), 1279m, 1157m (SO_4), 1109m, 1038m, 968m, 764m, 752m, 621m and 556w cm^{-1}. UV–VIS (DMF): 628 nm (ε 102 M^{-1} cm^{-1}).

$[CuBr_2(tpm)]\cdot 0.5H_2O$ 4 and $[Cu_2Br_3(tpm)_2]Br$ 5. A solution of tpm (0.24 g, 0.92 mmol) and $CuBr_2$ (0.20 g, 0.90 mmol) in methanol (25 cm^3) was boiled under reflux for 10 min, then concentrated to *ca.* 5 cm^3 *in vacuo.* The precipitate was filtered off as $[CuBr_2(tpm)]\cdot 0.5H_2O$ **4** (0.36 g, 83%). IR: 3347w and 3285w (NH_2), 1586m (py ring), 1163m, 1118m, 1017m, 936m, 851m, 772m, 760m, 746m, 650m and 635w cm^{-1}. UV–VIS (MeOH): 709 (133) and 261 nm (ε 17600 M^{-1} cm^{-1}).

Slow evaporation of a methanol solution of complex **4** in an open tube gave crystals of $[Cu_2Br_3(tpm)_2]Br\cdot 3H_2O$ **5**, which were used for X-ray crystallography. IR: 3285w (NH_2), 3171w, 1591m (py ring), 1290w, 1163m, 1018m, 773m, 756m, 654m, 638w and 507w cm^{-1}. UV–VIS (acetone): 713 (254) and 464 nm (ε 707 M^{-1} cm^{-1}).

$[Cu(tpm)_2][BF_4]_2\cdot Me_2CO$ 6, $[Cu(tpm)_3][BF_4]_2$ 7, $[Cu(tpma)_2][BF_4]_2$ 9 and $[Cu(tpml)_2][BF_4]_2$ 12. A solution of tpm (0.30 g, 1.1 mmol) and $Cu(BF_4)_2\cdot xH_2O$ (0.13 g, *ca.* 0.43 mmol) in ethanol (30 cm^3) was stirred for 5 h. The precipitate was filtered off, washed with ethanol, and dried *in vacuo* as $[Cu(tpm)_3][BF_4]_2$ **7** (0.32 g, 82%). IR: 3335w, 3279w and 3225w (all NH_2), 1587m, 1574m and 1558m (all py ring), 1173m, 1047 (s, BF_4), 995m, 789m, 777s, 751s and 519m cm^{-1}. UV–VIS (MeCN): 606 (80) and 259 nm (ε 34700 M^{-1} cm^{-1}).

Addition of acetone to the green complex **7** resulted in momentary dissolution, followed by rapid precipitation of a blue product, which was filtered off, washed with acetone and dried *in vacuo* as $[Cu(tpm)_2][BF_4]_2\cdot Me_2CO$ **6** (*ca.* 76%). IR: 3302m and 3248m (NH_2), 1705m (acetone), 1591m and 1572w (py ring), 1310m, 1165m, 1061s (BF_4), 802w, 768m, 189m, 754m, 671m and 590m cm^{-1}. UV–VIS (MeCN): 612 (111) and 260 nm (ε 24900 M^{-1} cm^{-1}). Slow evaporation of an acetone solution of **6** in an open tube gave crystals suitable for X-ray diffraction.

The experiment was repeated with tpma instead of tpm to give $[Cu(tpma)_2][BF_4]_2$ **9** (74%). IR: 3394m (NH), 1695s (amide I), 1597m (py ring), 1267m, 1074s (BF_4), 775m, 752m, 673m, 556m, 442m and 426m cm^{-1}. UV–VIS (MeCN): 573 (28) and 262 nm (ε 23900 M^{-1} cm^{-1}). Diffusion of diethyl ether into a solution of **9** in acetonitrile gave X-ray quality crystals.

Repetition of the experiment with tpml rather than tpm gave, after evaporation to dryness, extraction of the residue with dichloromethane and precipitation with ether, $[Cu(tpml)_2][BF_4]_2$ **12** (72%). IR: 3383m (NH), 1682s (amide I), 1597m and 1576m (py ring), 1290w, 1215w, 1082s (BF_4), 1005w, 770s, 667m, 625m, 521w and 444w cm^{-1}. UV–VIS (MeCN): 583 nm (ε 32 M^{-1} cm^{-1}).

$[Cu(OAc)_2(tpm)]\cdot 0.5CH_2Cl_2$ 8. A solution of $[Cu_2(OAc)_4(H_2O)_2]$ (0.22 g, 0.55 mmol) in warm ethanol (10 cm^3) was added to a solution of tpm (0.30 g, 1.14 mmol) in ethanol (10 cm^3), and allowed to evaporate to dryness overnight. The residue was dissolved in acetone, filtered, and ether added to the filtrate. The resulting precipitate was recrystallised from CH_2Cl_2–ether and dried *in vacuo* as $[Cu(OAc)_2(tpm)]\cdot 0.5CH_2Cl_2$ **8** (0.43 g, 84%). IR: 3412m, 3273m, 1587s and 1574s (CO_2 + py ring), 1335m, 1159w, 1028m, 995w, 781m, 721w, 671m and 619w cm^{-1}. UV–VIS (MeOH): 615 (102) and 262 nm (ε 17000 M^{-1} cm^{-1}).

$[Cu(tpms)_2]\cdot 4H_2O$ 10 and $[Cu(tpmb)_2]\cdot 3H_2O$ 11. A solution of $[Cu_2(OAc)_4(H_2O)_2]$ (0.055 g, 0.14 mmol) in a little water was added to a warm solution of tpmsH (0.20 g, 0.552 mmol) in 1 : 1 ethanol–water (20 cm^3). The mixture was evaporated to small volume in a nitrogen stream, then filtered, and the solid was dissolved in water. The solution was filtered, and acetone added to the filtrate until the first permanent precipitate was observed. The mixture was kept overnight, and the precipitate was filtered off as $[Cu(tpms)_2]\cdot 4H_2O$ **10** (0.11 g, 47%). IR: 3352m, 3271m, 1686m (amide I), 1597m (py ring), 1564m (CO_2), 1202w, 1161w, 1028w, 1007w, 777m, 721w and 573w cm^{-1}. UV–VIS (MeOH): 587 (30) and 260 nm (ε 24400 M^{-1} cm^{-1}). X-Ray quality crystals were obtained overnight by careful dilution of an aqueous solution of complex **10** with acetone until the first permanent precipitate was observed.

A similar reaction with tpmbH rather than tpmsH gave, by direct precipitation, $[Cu(tpmb)_2]\cdot 3H_2O$ **11** (79% yield). IR: 3603m, 3479m, 1647s (amide I), 1597m (py ring), 1541m, 1298m, 1244m, 1184m, 1086w, 1020m, 799w, 766m, 615m and 559m cm^{-1}.

$[Cu(SO_4)(tpml)(H_2O)]\cdot 0.5H_2O$ 13. A solution of $CuSO_4\cdot 5H_2O$ (0.11 g, 0.44 mmol) in the minimum of water was added to a solution of tpml (0.20 g, 0.45 mmol) in ethanol (10 cm^3). The mixture was evaporated to dryness under a nitrogen stream, then the residue was dissolved in a little ethanol. The solution was filtered and hexane added to the filtrate, which was kept at −10 °C overnight. The precipitate was filtered off and dried *in vacuo* as $[Cu(SO_4)(tpml)(H_2O)]\cdot 0.5H_2O$ **13** (0.15 g, 53%). IR: 3572m, 3246m, 3202m, 1693m (amide I), 1599m (py ring), 1528m (amide II), 1244w, 1175s, 1113s (SO_4), 1034s, 982m, 889w, 754m, 611m and 426w cm^{-1}. UV–VIS (MeCN): 617 (90) and 269 nm (ε 15400 M^{-1} cm^{-1}).

$[Cu_3(OAc)_4(mops)_2(H_2O)_2]\cdot CH_2Cl_2$ 14. A solution of $[Cu_2(OAc)_4(H_2O)_2]$ (0.13 g, 0.33 mmol) and mopsH (0.28 g, 0.71 mmol) in hot ethanol (30 cm^3) was stirred for 10 min, then filtered. The filtrate was concentrated *in vacuo* and ether added; the solid was filtered off and dried *in vacuo*. The crude product was dissolved in dichloromethane; addition of ether followed by filtration gave a solid which was dried *in vacuo* as $[Cu_3(OAc)_4(mops)_2(H_2O)_2]\cdot CH_2Cl_2$ **14** (0.17 g, 58%). IR: *ca.* 3337m, br (H_2O), 1686m (amide I), 1599s and 1572s (CO_2 + py ring), 1304m, 1267m, 1159m, 1028m, 768m and 675 cm^{-1}. UV–VIS (MeCN + 10% water): 620 (79) and 268 nm (ε 18600 M^{-1} cm^{-1}).

$[Cu(OAc)(bops)]\cdot 0.5CH_2Cl_2$ 15. A solution of $[Cu_2(OAc)_4(H_2O)_2]$ (0.080 g, 0.20 mmol) in a little water was added to a solution of bopsH (0.23 g, 0.54 mmol) in 1 : 1 ethanol–water (20 cm^3). The mixture was stirred for 2 min, then filtered. The filtrate was stirred for 2 h, then concentrated to dryness *in vacuo.* The residue was stirred with dichloromethane; the resulting solution was filtered and diluted with ether, giving a precipitate which was filtered off, washed with ether and dried *in vacuo* as $[Co(OAc)(bops)]\cdot 0.5CH_2Cl_2$ **15** (0.033 g, 14%). IR: 3344w (NH), 1680m (amide I), 1574s, br (CO_2 + py ring), 1308m, 1265m, 1155w, 1028m, 989w, 799m and 768m cm^{-1}. UV–VIS (MeOH): 673 (148) and 280 nm (ε 19500 M^{-1} cm^{-1}).

$[Cu(OAc)(tpms)(H_2O)]$ 16. A solution of $[Cu_2(OAc)_4(H_2O)_2]$ (0.11 g, 0.28 mmol) and tpmsH (0.21 g, 0.57 mmol) in ethanol (20 cm^3) was stirred for 10 min, then filtered and concentrated under a nitrogen stream. Ether was added and the mixture stirred for 30 min, then filtered. The residue was dissolved in boiling acetonitrile; the solution was filtered, concentrated and diluted with ether. The precipitate was filtered off, washed with ether and dried *in vacuo* as $[Cu(OAc)(tpms)(H_2O)]$ **16** (0.12 g, 45%). IR: 3390m, br (H_2O), 1684m (amide I), 1595s (CO_2 + py ring), 1300m, 1163m, 1024m, 758m and 664m cm^{-1}. UV–VIS (DMF): 658 (98) and 336sh nm (ε 1310 M^{-1} cm^{-1}).

$[Cu_4(SO_4)_4(bop)_3]$ 17. A solution of $CuSO_4 \cdot 5H_2O$ (0.15 g, 0.60 mmol) in water (5 cm^3) was added to a solution of bop (0.20 g, 0.62 mmol) in methanol (10 cm^3), and the solvent allowed to evaporate to dryness overnight. The residue was triturated with acetone, then filtered off, dried, and dissolved in acetonitrile. The solution was filtered and diluted with ether to give a precipitate, which was filtered off, washed with ether and dried *in vacuo* as $[Cu_4(SO_4)_4(bop)_3]$ **17** (0.055 g, 23%). IR: 3215m, 3080m, 1603s and 1574s (py ring), 1325m, 1271s, 1117s (SO_4), 1028s, 988m, 802m, 772m, 721w, 656w and 604m cm^{-1}. UV–VIS (MeOH): 664 (79), 358sh (1650) and 263 nm (ε 15000 M^{-1} cm^{-1}).

$[\{Cu(SO_4)(mde)\}_2]\cdot 3H_2O$ 18 and $[Cu(SO_4)(mde)(H_2O)]\cdot 0.5H_2O$ 19. A solution of $CuSO_4 \cdot 5H_2O$ (1.00 g, 4.0 mmol) in water (10 cm^3) was added to a stirred solution of mde (0.994 g, 4.1 mmol) in methanol (40 cm^3). The mixture was stirred for 5 h, then concentrated *in vacuo*, to give an oil. This was stirred with acetone and the resulting solid filtered off, dried, and extracted with methanol. Filtration gave a turquoise solid A plus a dark green filtrate B. Solid A was dissolved in wet methanol, and acetone was added to the filtrate until the first permanent precipitate. The mixture was kept at −10 °C overnight, then decanted and the decantate concentrated to dryness *in vacuo.* The residue was recrystallised from wet methanol–acetone as above as $[\{Cu(SO_4)(mde)\}_2]\cdot 3H_2O$ **18** (0.42 g, 25%). IR: 3370w and 3205w (NH), 1593m and 1570w (py ring), 1165m, 1086s (SO_4), 1026m, 764w, 721w and 606m cm^{-1}. UV–VIS (water): 657 nm (ε 36 M^{-1} cm^{-1}). X-Ray quality crystals were obtained overnight by diluting a solution of complex **18** in methanol–water with acetone.

Filtrate B was concentrated to dryness *in vacuo*, and the residue dissolved in the minimum of methanol. The solution was filtered and excess of ether was added to the filtrate. The precipitate was filtered off, washed with ether and dried *in vacuo* as $[Cu(SO_4)(mde)(H_2O)]\cdot 0.5H_2O$ **19** (0.70 g, 40%). IR: 3396w and 3217w (NH), 1605m and 1572w (py ring), 1117s (SO_4), 1032m, 972m, 777m, 721w and 613m cm^{-1}. UV–VIS (MeOH): 671 (83), 360 (2310) and 261 nm (ε 11200 M^{-1} cm^{-1}).

$[Zn(tpm)(H_2O)_3]_2[Zn(H_2O)_6][SO_4]_3\cdot 3H_2O$ 20. tpm (1.11 g, 6.0 mmol) was dissolved in methanol (100 cm^3). To the warm solution was added dropwise a solution of $ZnSO_4 \cdot 7H_2O$ (1.73 g, 6.0 mmol) in water (20 cm^3). The solution was heated gently for 30 min, then filtered whilst still hot and allowed to cool in an open beaker. The white precipitate was collected by filtration, washed with two 5 cm^3 portions of ethanol, followed by 5 cm^3 of diethyl ether, and air-dried as $[Zn(tpm)(H_2O)_3]_2[Zn(H_2O)_6][SO_4]_3\cdot 3H_2O$ **20** (1.62 g, 63%) (Found: C, 30.3; H, 4.6; N, 8.8. Calc. for $C_{32}H_{52}N_8O_{24}S_3Zn_3\cdot 3H_2O$: C, 30.0; H, 4.6; N, 8.8%). UV–VIS (water): 269 (34800) and 262 nm (ε 38400 M^{-1} cm^{-1}). Λ_M(water): 501 S cm^2 mol^{-1}. IR: 3385m (br, H_2O), 3265w, 1595m (py ring), 1464m, 1441m, 1109s, br (SO_4^{2-}), 1020m, 773m, 758m, 656m, 640m and 617m cm^{-1}. Several crops having identical IR spectra were obtained. Crystals suitable for X-ray crystallography were grown by slow diffusion of 2-propanol into a saturated aqueous solution.

$[Cu(tpm)(NCMe)]PF_6\cdot 0.33Et_2O$ 21. Dry acetonitrile (20 cm^3) was added to a solid mixture of tpm (0.2 g, 0.76 mmol) and $[Cu(NCMe)_4]PF_6$ (0.28 g, 0.76 mmol), and the resulting solution was stirred for 5 h, then concentrated *in vacuo* to *ca.* 5 cm^3. Addition of ether gave a precipitate, which was isolated by Schlenk filtration. The crude product was recrystallised from acetonitrile–ether as $[Cu(tpm)(NCMe)]PF_6\cdot 0.33Et_2O$ **21** (0.33 g, 81%). ^{1}H NMR (CD_3CN): δ 8.57 (br m, 3H, H^6), 7.85 (br m, 3H, H^4), 7.41 (br m, 3H, H^3), 7.13 (br m, 3H, H^5), 4.20 (br, 2H, NH_2) and 1.95 (s, 3H, CH_3CN); spectrum also shows ether in the correct ratio. ^{13}C-{^{1}H} NMR (CD_3CN): δ 161.3 (C^2), 150.1

Table 3 Crystallographic and refinement data for the copper and zinc complexes

	[Cu(tpm)(H$_2$O)(SO$_4$)]·3H$_2$O **1**	[{Cu(tpm)}$_2$Br$_3$]Br·3MeOH **5**	[Cu(tpm)$_2$][BF$_4$]$_2$·Me$_2$CO **6**	[Cu(tpma)$_2$][BF$_4$]$_2$ **9**	[Cu(tpms)$_2$]·8H$_2$O **10**	[{Cu(SO$_4$)(mde)}$_2$]·3H$_2$O **18**	[Zn(tpm)(H$_2$O)$_3$]$_2$[Zn(H$_2$O)$_6$][SO$_4$]$_3$·3H$_2$O **20**
Elemental formula	$C_{16}H_{16}CuN_4O_5S\cdot 3H_2O$	$C_{32}H_{28}Br_4Cu_2N_8\cdot 3CH_4O$	$C_{32}H_{28}B_2CuF_8N_8\cdot C_3H_6O$	$C_{36}H_{32}B_2CuF_8N_8O_2$	$C_{40}H_{34}CuN_8O_6\cdot 8H_2O$	$C_{26}H_{30}Cu_2N_6O_8S_4\cdot 3H_2O$	$C_{32}H_{52}N_8O_{24}S_3Zn_3\cdot 3H_2O$
M	494.0	1067.5	819.9	845.9	930.4	863.9	1279.2
Crystal system	Orthorhombic	Orthorhombic	Monoclinic	Orthorhombic	Monoclinic	Monoclinic	Monoclinic, twinned
Space group (no.)	$Pna2_1$ (33)	*Pnmm* (equiv. to 59)	*A*2/*a* (equiv. to 15)	*Pbca* (61)	$P2_1/n$ (equiv. to 14)	$P2_1/n$ (equiv. to 14)	$P2_1/a$ (equiv. to 14)
a/Å	13.729(3)	8.1466(14)	15.8308(14)	11.714(2)	14.7630(12)	9.1541(14)	16.536(2)
b/Å	8.0736(9)	14.188(2)	10.8103(12)	13.828(2)	11.180(2)	13.264(2)	13.789(2)
c/Å	17.869(2)	31.992(5)	22.990(2)	23.072(3)	14.511(2)	14.255(4)	22.407(2)
β/°	90	90	111.259(8)	90	117.133(8)	95.24(2)	111.652(8)
V/Å^3	1980.7(5)	3697.8(10)	3666.6(6)	3737.0(9)	2131.5(4)	1723.7(6)	4748.6(9)
Z	4	4	4	4	2	2	4
μ(Mo-Kα)/cm^{-1}	12.6	55.2	6.78	6.70	5.90	15.4	17.36
Total no. reflections measured (not including absences)	2858	6014	3588	3657	4876	4859 (to θ = 26°)	11830
Total no. unique reflections	2457	3461	3211	3657	4176	3374 (2712 to θ = 24°)	11434
R_{int} for equivalents	0.019	0.100	0.016	—	0.025	0.081	0.012
Final $R1$ (all data)	0.065	0.107 (2395 with $I > \sigma_I$)	0.058	0.144	0.057	0.079 (2712)	0.054
$wR2$ (all data)	0.139	0.217 (2396 with $I > \sigma_I$)	0.086	0.159	0.122	0.118 (2712)	0.115
$R1$ for 'observed' data	0.054	0.073	0.036	0.054	0.041	0.049	0.044
No. 'observed' reflections ($I > 2\sigma_I$)	1963	1490	2284	1450	3111	1798 (to θ = 24°)	9411

(C^6), 138.4 (C^4), 124.5 (C^3) and 70.9 (CNH_2). ^{31}P NMR (CD_3CN): δ −285.5 (s, $J_{PF} = 706$ Hz, PF_6^-). IR: 3389w and 3330w (NH_2), 1587m (py ring), 1149m, 1114m, 1013m, 962m, 901m, 838s (PF_6), 770m, 752m, 651m, 635m, 555m, 489w and 418m cm^{-1}.

Crystal structure analyses

The crystal structure analysis of $[Cu(SO_4)(tpm)(H_2O)]\cdot 3H_2O$ **1** is described here. The other compounds were examined by very similar procedures. Crystallographic and refinement data for all the complexes are collated in Table 3, and further crystallographic features are included below; all intensity data were measured at 293 K.

Crystals of complex **1** were thick, turquoise plates. One, mounted on a glass fibre, was examined photographically, then transferred to an Enraf-Nonius CAD4 diffractometer (with monochromated radiation) for determination of accurate cell parameters and for measurement of diffraction intensities. During processing, corrections were applied for Lorentz-polarisation effects, absorption (by semi-empirical ψ-scan methods) and to eliminate negative net intensities (by Bayesian statistical methods). No deterioration correction was necessary. The structure was determined by the direct methods routines in the SHELXS program[20] and refined by full-matrix least-squares methods on F^2 in SHELXL.[21] Hydrogen atoms on the pyridyl rings were included in idealised positions; the two amino hydrogens were located in a difference map and refined with geometrical constraints. The isotropic thermal parameters of all hydrogen atoms were allowed to refine freely. The sulfate ligand is disordered in two orientations, sharing a common site for the coordinated oxygen atom. Four water molecules were identified, one bound to the copper atom, and three as free solvent molecules; two of these last are disordered over pairs of sites with the same ratio of major : minor occupancies (0.65 : 0.35) as for the sulfate ligand. The non-hydrogen atoms (except for the minor components of the solvent oxygens) were refined with anisotropic thermal parameters.

Scattering factors for neutral atoms were taken from reference 22. Computer programs used in this analysis have been noted above or in Table 4 of reference 23, and were run on a DEC-AlphaStation 200 4/100 in the Department of Biological Chemistry, John Innes Centre.

Crystals of $[Zn(tpm)(H_2O)_3]_2[Zn(H_2O)_6][SO_4]_3\cdot 3H_2O$, **20**, were twinned, with one twin's diffraction pattern superimposed precisely on that of the second twin. Data for the composite crystal were recorded and, using the TWIN/BASF routines in SHELXL, the structure of each twin was determined and refined well; the refinement of BASF showed that the ratio of twins was *ca.* 62 : 38.

CCDC reference number 186/2326.

See http://www.rsc.org/suppdata/dt/b0/b008476j/ for crystallographic files in .cif format.

Acknowledgements

We thank the BBSRC for financial support for this work, and EPSRC for a ROPA award (to P. C. S.). Dr M. Cocksedge is thanked for help with mass spectra.

References

1 S. Trofimenko, *Chem. Rev.*, 1993, **93**, 943.
2 D. L. Reger, *Comments Inorg. Chem.*, 1999, **21**, 1.
3 L. F. Szczepura, L. M. Witham and K. J. Takeuchi, *Coord. Chem. Rev.*, 1998, **174**, 5, and references therein.
4 V. Levacher, H. Adolfsson and C. Moberg, *Acta Chem. Scand.*, 1996, **50**, 454.
5 R. T. Jonas and T. D. P. Stack, *Inorg. Chem.*, 1998, **37**, 6615.
6 J. W. Godden, S. Turley, D. C. Teller, E. T. Adman, M. Y. Liu, W. J. Payne and J. Le Gall, *Science*, 1991, **253**, 438; E. T. Adman, J. W. Godden and S. Turley, *J. Biol. Chem.*, 1995, **270**, 27458.
7 F. E. Dodd, J. Van Beeumen, R. R. Eady and S. S. Hasnain, *J. Mol. Biol.*, 1998, **282**, 369.
8 S. Suzuki, K. Kataoka, K. Yamaguchi, T. Inoue and Y. Kai, *Coord. Chem. Rev.*, 1999, **190–192**, 245.
9 W. Kaim and J. Rall, *Angew. Chem., Int. Ed. Engl.*, 1996, **35**, 43.
10 K. Djinovic, G. Gatti, A. Coda, L. Antolini, G. Pelosi, A. Desideri, M. Falconi, F. Marmocchi, G. Rotilio and M. Bolognesi, *J. Mol. Biol.*, 1992, **225**, 791; W. R. Rypniewski, S. Mangani, B. Bruni, P. L. Orioli, M. Casati and K. S. Wilson, *J. Mol. Biol.*, 1995, **251**, 282.
11 A. J. Blake, S. J. Hill, P. Hubberstey and W. S. Li, *J. Chem. Soc., Dalton Trans.*, 1998, 909.
12 P. Arnold, S. C. Davies, J. R. Dilworth, M. C. Durrant, D. V. Griffiths, D. L. Hughes and R. L. Richards, *Inorg. Chem. Commun.*, 1998, **1**, 43.
13 E. Niemers and R. Hiltmann, *Synthesis*, 1976, 593; M. Renz, C. Hemmert and B. Meunier, *Eur. J. Org. Chem.*, 1998, **7**, 1271.
14 M. Kodera, Y. Tachi, T. Kita, H. Kobushi, Y. Sumi, K. Kano, M. Shiro, M. Koikawa, T. Tokii, M. Ohba and H. Okawa, *Inorg. Chem.*, 2000, **39**, 226.
15 Y. Fujii, Z. Wang, R. D. Willett, W. Zhang and C. P. Landee, *Inorg. Chem.*, 1995, **34**, 2870; D. M. Nilsen, R. D. Larsen, K. Emerson, G. V. Rubenacker, Z. Ping and J. E. Drumheller, *Inorg. Chem.*, 1990, **29**, 2887; S. A. Roberts, D. R. Bloomquist, R. D. Willett and H. W. Dodgen, *J. Am. Chem. Soc.*, 1981, **103**, 2603.
16 P. V. Berhardt, P. Comba, A. Mahu-Rickenbach, S. Stebler, S. Steiner, K. Várnagy and M. Zehnder, *Inorg. Chem.*, 1992, **31**, 4149.
17 M. C. Munoz, J. M. Lazaro, J. Faus and M. Julve, *Acta Crystallogr., Sect. C*, 1993, **49**, 1756.
18 S. C. Davies, J. R. Dilworth, M. C. Durrant, D. V. Griffiths, D. L. Hughes, R. L. Richards and P. C. Sharpe, to be published.
19 D. F. Shriver, *Inorg. Synth.*, 1979, **19**, 90.
20 G. M. Sheldrick, *Acta Crystallogr., Sect. A*, 1990, **46**, 467.
21 G. M. Sheldrick, SHELXL, Program for Crystal Structure Refinement, University of Göttingen, 1993.
22 *International Tables for X-Ray Crystallography*, Kluwer Academic Publishers, Dordrecht, 1992, vol. C, pp. 193, 219 and 500.
23 S. N. Anderson, R. L. Richards and D. L. Hughes, *J. Chem. Soc., Dalton Trans.*, 1986, 245.
24 W. J. Geary, *Coord. Chem. Rev.*, 1971, **7**, 81.